EPJ Web of Conferences **250**, 06002 (2021) https://doi.org/10.1051/epjconf/202125006002
DYMAT 2021

Size Dependence and Dynamic Properties of Adobe Masonry Bricks tested at high strain rates

T. Li Piani[1], J. Weerheijm[1,2], M. Peroni[3], L.J. Sluys[1]

1 TU Delft, Stevinweg 1, 2628 CN Delft, The Netherlands
2 TNO – Defence, Safety and Security, The Hague, The Netherlands
3 European Commission, Joint Research Centre (JRC), Ispra, Italy

Abstract. Masonry is a construction technique which typically reacts in compression. Characterization of its material properties in compression is thus of paramount importance. This especially counts for adobe bricks because their material properties are still unknown to a large extent. This traditional masonry, made of locally available soil and fibres, is spread in areas currently involved in military conflicts, where also European forces operate. Therefore, not only its static properties in compression, but even more the dynamic strength is a relevant parameter. Laboratory characterization of material properties still pose several challenges, among which so-called size dependence is one of the most controversial topics. This entails the possible variation of material properties values from tests on specimens of different size and shape. Several factors may concur to its determination and a well-founded theory does not exist yet. This counts for statics and even more in dynamics. Addressing the properties in compression of bricks at high strain rates is rare, namely no studies of size dependence on masonry bricks in dynamic regimes are published. Lately, a series of experimental campaigns were conducted by the authors at the Joint Research Centre of the European Commission. In these campaigns, a series of compression tests were performed on several types of adobe bricks. Different soil mixtures were used to produce cylindrical samples of different sizes. Compressive tests from $2e^{-5}$ s^{-1} to 10 s^{-1} and 100 s^{-2} were executed using hydraulic machines as well as split Hopkinson bars. Next, the static as well as the dynamic material properties as calculated from tests on specimens of different sizes and material compositions have been qualitatively and quantitatively compared and interpreted. In this paper, the experimental program is presented, next the material properties in strength and ductility as well as the dynamic increase factors are investigated.

1 Introduction

An increasing number of military operations is taking place in highly urbanized environments located out of area (OoA-Out of Area Operations). In these contexts, battle fields are displayed among houses and structures for civilian use. In many countries, these houses are still not engineered, namely the material properties, manufacture process, building technology have not been standardized yet. This especially counts for ancient masonry technologies as adobe. Adobe connotes a building technique characterized by the use of locally available soil to produce both bricks and mortar, possibly adding fibres to the soil mixture to prevent shrinkage cracks during sun drying curing process [1]. Even the static properties of adobe are largely unknown, and this especially counts when heterogeneity in

the micro-structure of the masonry components increases adding fibres [2]. Furthermore, production and construction processes are still delegated to local owners in the field, with the consequence of the overall quality and building-applicability of the final product which should be ensured by standard codes. Actually, some building codes devoted to adobe already exist around the world. Only two of them addresses the topic of size dependence by introducing aspect ratio dependent functions. However, these functions have not been validated against the plethora of tests executed over the recent past years in literature, nor account for the influence of shape and especially mixture composition on the static properties of bricks and mortar. Not only the static properties, but especially the dynamic performance of natural composite materials as adobe, counts. This is the case because adobe masonry structures are largely spread in many areas of the world currently involved into military operations [3]. These imply shooting attacks and close impact within wall breaching and sniper operations [4]. The assessment of the dynamic material properties such as the dynamic increase factor for adobe components is thus of paramount importance to develop engineering and numerical models that simulate highly dynamic events. If the static properties of adobe are still not completely addressed, experimental data on the dynamic performance are even more rare [5]. This research aims to bridge the two knowledge gaps just presented. This paper presents and interprets the results of a series of experimental campaigns aimed at testing the static as well as the dynamic material properties of adobe specimens of different size, shape and material composition. Cylindrical and prismatic samples were extracted from two brick batches made of the same soil composition but with only one mixed using natural fibres. Series of compressive tests were executed. Three different strain rates were applied, namely static tests, and dynamic impact tests at strain rates of $3s^{-1}$ and $100s^{-1}$. Results collected in this paper are meant to help answer the following research questions for adobe: a) Influence of shape, size and fibres on static unconfined strength and validation of existing standard; b) Influence of size on the dynamic increase factors; c) Influence of fibres on the dynamic increase factors.

2 The experimental campaign

A series of joint experimental campaigns including Delft University of Technology (TU Delft), TNO – DSS (Defense, Safety and Protection), Dutch Ministry of Defence and the Joint Research Centre of the European Commission, were carried out over the past years to characterize the dynamic performance of adobe materials. In the following, materials used, specimen sizes and geometry, emplaced setup and main results are resumed.

2.1 Materials and Specimens

Two types of adobe bricks (named A and B in the following) were selected for testing. They resulted from the same soil but only one (Type B) of them contained substantial percentages (17-18%bv) of randomly distributed natural fibres of wood and straw (Fig. 1). Preliminary physical tests confirmed that both types of bricks approximately had the same water content (~2.3-2.4%). Specimens of cylindrical and prismatic shapes were drilled from both brick batches and rectified under the same laboratory conditions. Two cylindrical geometries (named I and II in the following), were designed, with an aspect ratio of 0.5 and 1, respectively. Prismatic samples (III) with square section and an aspect ratio of 2 were drilled as well. In details, I: Cylindrical, Dxh (110x55mm), aspect ratio= 0.5; II: Cylindrical, Dxh (40x40mm), aspect ratio= 1; III: Prismatic, bxt (45x90mm), aspect ratio= 2.

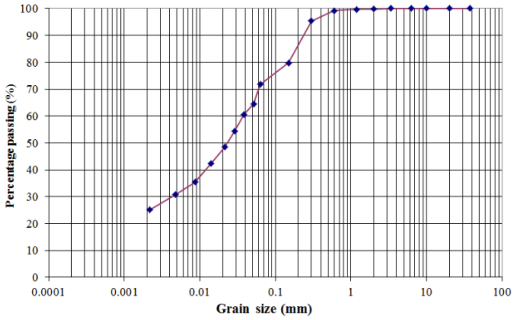

Fig. 1. Soil granulometry and fibres for the mixture

2.2 Test setup

2.2.1 Static Tests at 3 10^{-4} s^{-1}

Static tests were performed using an MTS universal testing machine. Two adjustable compression platens were used to correctly load the specimens in compression. Displacement controlled tests at a constant velocity were executed. For each specimen geometry, the velocity value of the platen was calibrated to achieve the same average strain rate. Strain rate values were calculated by dividing velocity by specimen length. Average strain rates of about 3 10^{-4} s^{-1} were obtained for all specimens. Displacement and forces during tests were recorded and average stress-strain plots were derived normalizing each curve over the corresponding cross section areas and heights. A camera was installed to acquire high resolution photo sequences at 1 frames/s (Fig. 2).

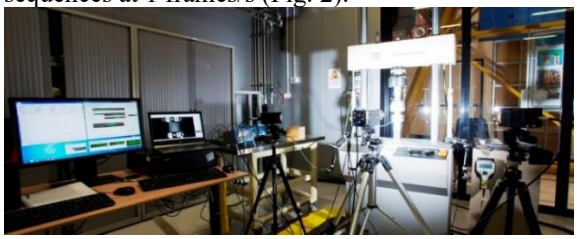

Fig. 2. Static test setup

2.2.2 Dynamic Tests at 3 s^{-1}

Dynamic tests were performed at two different strain rates, in the range corresponding to impact and blast . Tests at an intermediate strain rate were performed using the same setup and machine of Fig. 2, with two differences. Displacement controlled tests were performed to generate average strain rates in the specimens of about 3 s^{-1}. Normalized stress strain relations and failure modes were recorded.

2.2.3 Dynamic Tests at 120 s^{-1}

Dynamic test at approximately 100s^{-1} of strain rate were carried out using a modified Hopkinson bar at the Hop-Lab of JRC. The input and output bars of 40 mm diameter are made of aluminium. The input pulse is generated through the pre-stressing and abrupt release of a steel portion of the bar of 25 mm in diameter. Test setup is shown and machine scheme

are sketched in Fig.3. For a detailed report of the dynamic test machine, the reader is referred to [6]. In the tests, the incident bar applies a constant velocity of about 4200 mm/s to the sample. For each test, specimen loading conditions and corresponding bar ends displacements can be calculated by properly processing the strain signals recorded with a chain of semiconductor strain gages applied to the bars. For this purpose, a sample-rate of 5 MHz was used and the data acquisition system GAGE Module A/D Express CSE8482-H2 with dedicated software was employed. For each test, a thin layer of vaseline was applied at the interfaces between the bar end and the sample surfaces to minimize friction and maximise plane-parallelism. Moreover, samples were prestressed up to 5% of the static strength for clamping and horizontal positioning purposes. Time-synchronized high-resolution videos were recorded at 50,000 frames/s using the Photron SA1.1 digital camera. Image resolution is adequate to track failure patterns also in case of high velocity impacts.

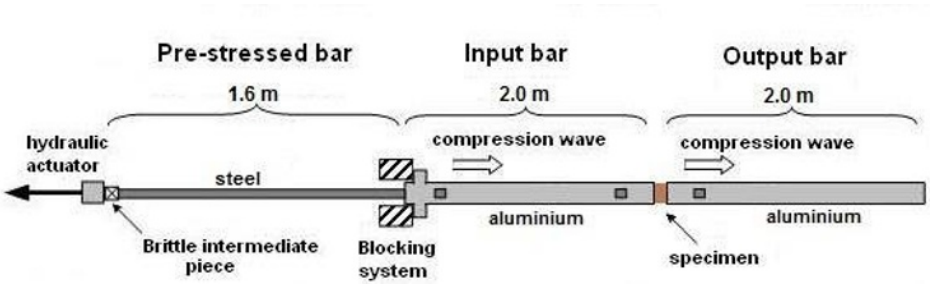

Fig. 3. Split Hokpinson Bar Test Setup

2.3 Test Program and Results

Static tests were executed on all specimen geometries and material types. Intermediate strain rate tests were executed on the two cylindrical specimens and material types. Cylindrical specimens of 40x40mm for both types were selected for the split Hopkinson bar tests. The following Tab.1 presents the results related to the assessment of the compressive strength. For each test series, the average value from at least 3 tests has been calculated.

Tab.1. Average values of compressive strength (in MPa) for each type and geometry tested at different rates. Standard deviation is consistently in the order of 0.1-0.2

Rate / Type	Static	$3s^{-1}$	$120s^{-1}$
A-I	4.4	5.4	-
B-I	2.6	3.4	-
A-II	2.6	3.1	4.8
B-II	1.4	1.7	2.3
A-III	3.0	-	-
B-III	1.3	-	-

3 Analysis of Results

3.1 The influence of geometry on the static properties of adobe

Values of the unconfined compressive strength for both material compositions are calculated from the three geometries tested. This is done using the aspect-ratio laws proposed for adobe in the Australian and New Zealand codes for adobe. Usually, codes for adobe suggest tests on large specimens (>200mm) with high slenderness (3-5), but also accept the usual standard slenderness for concrete elements of 2. In addition, also the typical size dependence law used in testing standard for concrete elements was used. Laws are shown in Fig.4 [7]–[9]. Corresponding values of the unconfined strengths are displayed for all geometries and both types in Fig.5.

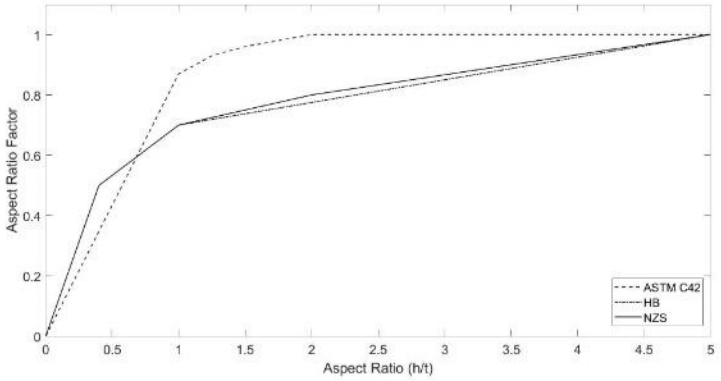

Fig. 4. Aspect ratio correction factors according to different standard (HB, NZS, ASTM)

Mean stress-strain relationships and corresponding values of unconfined strengths using the HB laws are also presented in Fig 6. From analysis, the HB aspect ratio laws seem to provide the closest size-independent results for a slenderness above 1, whereas the ASTM standard provides size-independent results up to a slenderness of 0.5. These correspond to the most conservative branches of the aspect ratio laws, respectively. Heterogeneity in the mixture is interpreted to play a major role on the overall material performance with respect to standardized concrete materials.

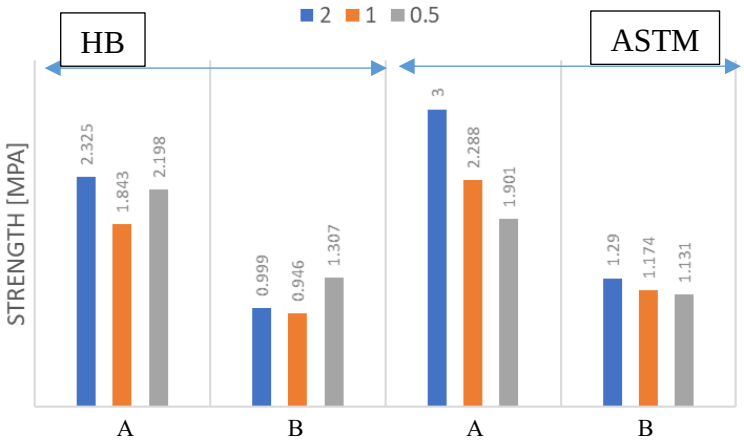

Fig. 5. Unconfined strength values for different material compositions geometry using HB and ASTM

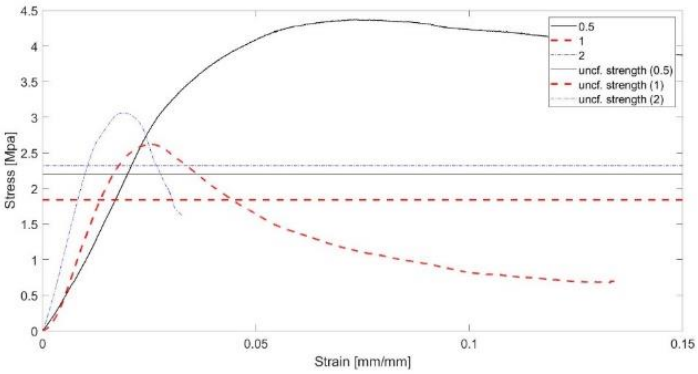

Fig. 6. Stress strain laws for type A (plain adobe) of three geometries and unconfined strengths levels according to HB aspect ratio laws

3.2 The influence of geometry on the dynamic properties of adobe

For the cylindrical geometry (I, II) in Tab.1, the mean values of the dynamic compressive strength of both types of adobe specimens have been used to determine a dynamic increase factor for adobe corresponding to strain rates of $3s^{-1}$. Values for the two types and geometries are shown in Tab.2. For both types, the dynamic increase factors derived from the two values for the slenderness appear to be similar. The DIF ranges between 1.2-1.3 for Type A and is about 1.2 for Type B. For both geometries, the DIF is lower for Type B with respect to corresponding values of Type A. Further analysis follows in Par. 3.3. In this paragraph, attention is paid to a common trend for both types, which corresponds to slightly higher DIF values for a slenderness of 1 (II) against a slenderness of 0.5 (I). The ratio between corresponding DIFs is equal to 1.1 for both types. This may be interpreted as the consequence of a confinement plate effect on thick specimens which enhances the static strength of the material. In fact, in statics, given a limited set of flaws inside the material, the most critically sized and oriented ones undergo crack initiation and propagation. As these microcracks approach the vicinity of other propagating ones, they may interact and coalesce into a macro crack which leads to loss of structural integrity and failure at a macro-scale. If propagating flaws encounter stiffer areas, they have the time to deviate around them bridging into macro-cracks and the fracture and stress path with minimum energy demand is taken. This interpretation is consistent with the need for the factor size correction functions depicted in Par. 3.1 to derive unconfined values of compressive strength.

Tab.2. Average values of the dynamic increase factor for the two slenderness

Type / DIF	A-I	A-II	B-I	B-II
Rate $3s^{-1}$	1.23	1.32	1.17	1.21

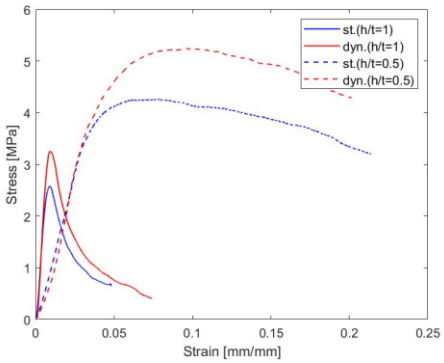

Fig. 7. Typical stress strain relationships in static (blue) and dynamic (red) for the two geometries of Type A

3.3 The influence of fibres on the dynamic properties of adobe

Dynamic increase factors on 40x40mm cylindrical specimens corresponding to $120s^{-1}$ strain rates have been calculated for both types of adobe. Average values of DIF functions including values in Par.3.2 are plotted for Type A and Type B in Fig. 8.The average DIF for Type A is about 1.84 at $120s^{-1}$, whereas it is 1.71 for Type B. From the plot, it appears that fibre reinforced adobe always corresponds to lower DIF functions.

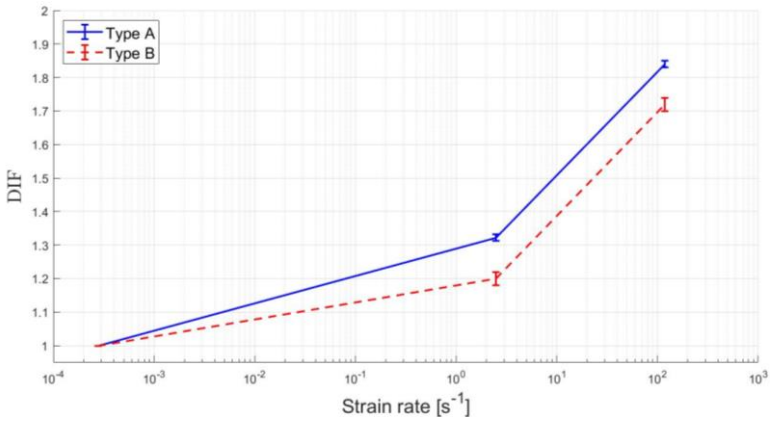

Fig. 8. DIF functions for Type A and Type B

The lower sensitivity of strength to high strain rates exhibited by adobe samples containing fibres is interpreted by linking principles of fracture mechanics to hypotheses on the specific heterogeneity level of fiber enriched mixtures of adobe [10]. Given the failure processes depicted in Par. 3.2. in static regimes, in dynamics, loading is characterized by a short time duration and high supply rates which forces simultaneous cracks at multiple spots also through the stiffer areas of the material. As a result, more diffuse systems of short and straight cracks initiated at multiple weak spots are often observed in quasi brittle materials such as concrete, corresponding to higher values for compressive strength and strain at peak strength. The theory of fracture mechanics hooks up the experimental evidence for adobe given that the rate of enhancement of the dynamic material properties depends on the spatial distributions of the micro-flaws inside the material, that is by the level of uniformity of a mixture. If the number of micro-flaws increases, the probability of interaction increases also in case of dynamic loading. It means that if density of initial flaws distribution is sufficiently high, the effect of loading rate on the crack bridging processes will be limited and a stress path with a energy demand close to statics can be observed also in the dynamic regime. This can explain the lower DIF value. This interpretation is also consistent with the depicted trends experimentally derived in Sec. 2 of lower strength values associated to bricks mixed with fibres in statics.

4 Conclusions

Compression tests in static and dynamic regimes have been performed on adobe specimens of different geometries, shapes and material composition. From analysis of results, the following conclusions for adobe are listed:

- The compressive strength of adobe is geometry (size and shape) dependent. The static compressive strength always increases with a lower slenderness. The lower envelope corresponding to the aspect ratio functions of NZS and ASTM is recommended to be used to calculate the unconfined compressive strength. It is interpreted that the geometry

dependence is higher than for standard concrete elements because of the enhanced heterogeneity at the micro-scale of the mixture.

- The compressive strength of adobe is rate dependent. DIF values at strain rates of 3s-1 for cylindrical specimens of 1 and 0.5 slenderness values are similar but slightly increase for lower slenderness. This is interpreted as the consequence of a plate confinement effect exerted in statics.

- DIF values at strain rates ranging from 10-3 s-1 to 120 s-1 for cylindrical specimens with slenderness 1 decrease with the introduction of fibres in the mixture. This is interpreted as the result of an enhanced porosity determined by fibre introduction. Adding fibres in the mixture enhances the heterogeneity of the material for adobe and fibres weaken interparticle bonds in the matrix causing the presence of weak regions at a meso-scale.

References

[1] F. Pacheco-Torgal and S. Jalali, "Earth construction: Lessons from the past for future eco-efficient construction," *Constr. Build. Mater.*, vol. 29, pp. 512–519, 2012, doi: 10.1016/j.conbuildmat.2011.10.054.

[2] T. Li Piani, D. Krabbenborg, J. Weerheijm, L. Koene, and L. Sluys, "The Mechanical Performance of Traditional Adobe Masonry Components: An experimental-analytical characterization of soil bricks and mud mortar (in submission)," 2017.

[3] T. Li Piani, J. Weerheijm, L. Koene, and L. J. Sluys, "The Ballistic Resistance of Adobe Masonry : An analytical model for impacts on mud bricks and mortar," in *The 17th International Symposium on the Interaction of the Effects of Munitions with Structures (17th ISIEMS)*, 2017, no. October.

[4] T. Li Piani, J. Weerheijm, and L. J. Sluys, "Ballistic model for the prediction of penetration depth and residual velocity in adobe: A new interpretation of the ballistic resistance of earthen masonry," *Def. Technol.*, vol. 14, no. 5, pp. 4–8, 2018, doi: https://doi.org/10.1016/j.dt.2018.07.017.

[5] T. Li Piani *et al.*, "Dynamic behaviour of Adobe bricks in compression: the role of fibres and water content at various loading rates," *Constr. Build. Mater.*, vol. 230, no. October, pp. 117–135, 2020.

[6] M. Peroni, G. Solomos, and N. Babcsan, "Development of a Hopkinson bar apparatus for testing soft materials: Application to a closed-cell aluminum foam," *Materials (Basel).*, vol. 9, no. 1, 2016, doi: 10.3390/ma9010027.

[7] NZS 4298, "NZS 4298 (1998): Materials and workmanship for earth buildings," *New Zeal. Tech. Committe*, vol. 4298, p. 91, 1998.

[8] *HB 195 - The Australian earth building handbook-Standards Australia International, NSW 2001*. 2001.

[9] "ASTM C1314-16: Standard Test Method for Compressive Strength of Masonry Prisms." .

[10] T. L. Piani, J. Weerheijm, and L. J. Sluys, "Dynamic simulation of traditional masonry materials at different loading rates using an enriched damage delay : theory and practical applications," 2019.